



Research Article

UPSCALING RESULTS FROM OPTIMUM SALINITY WATERFLOODING AT THE CORE SCALE TO A 3D DYNAMIC GRID

Authors: David ALAIGBA , Onaiwu D. ODUWA , Olalekan OLAFUYI , Ismaila MOHAMMED 

To cite to this article: Alaigba, D., Oduwa, O., Olafuyi, O. Mohammed, I., (2022). Upscaling Results from Optimum Salinity Waterflooding at the Core Scale to a 3D Dynamic Grid. International Journal of Engineering and Innovative Research , 4(2), p:114-125 . DOI: 10.47933/ijeir.1098565

DOI: 10.47933/ijeir.1098565

To link to this article: <https://dergipark.org.tr/tr/pub/ijeir/archive>



International Journal of Engineering and Innovative Research

<http://dergipark.gov.tr/ijeir>

UPSCALING RESULTS FROM OPTIMUM SALINITY WATERFLOODING AT THE CORE SCALE TO A 3D DYNAMIC GRID

David ALAIGBA¹, Onaiwu D. ODUWA¹, Olalekan OLAFUYI¹, Ismaila MOHAMMED¹

¹University of Benin, Faculty of Engineering, Petroleum Engineering, Benin-City, Nigeria

<https://doi.org/10.47933/ijeir.1098565>

*Corresponding Author: david.alaigba@gmail.com
(Received: 04.04.2022; Accepted: 07.06.2022)

ABSTRACT: In order to fully quantify the volumes in place, capture the dynamics of fluid flow, production forecast and consequently economic potentials of oil and gas reservoirs, 3-dimensional (3D) models filled with relevant rock, fluid parameters and well information are built. This work carried out Optimum Salinity core flooding (OPTSWF) with progressive dilution of the invading brine at the laboratory scale. Next, the relative permeability curves for oil and water for the initial and final salinity conditions were obtained using Corey's estimation. These curves were then loaded into a 3D dynamic model and the model was run under different salinity conditions to quantify the incremental oil recovery from Optimum Salinity Waterflooding and to visualize the process in 2D. Interestingly, the impact of optimizing the salinity was visibly seen in the 3D grid results and helped to visually explain the observed additional recovery from the OPSWF experiment.

Keywords: Core Flooding, Optimum Salinity Water Flooding, 3D Reservoir Model, Low Salinity Waterflooding, Corey, Improved Oil Recovery

1. INTRODUCTION

Ensuring energy security for the future generations is a critical topic in the continuously growing world as the global population continuously grows. According to [1], the petroleum reserves in the Niger Delta has peaked due to limited or highly reduced exploration activities which is occasioned by multiple factors which are not limited to; low oil price, global Covid-19 pandemic, political instability, and uncertainty surrounding the passage of the Petroleum Industry Bill, PIB. An interesting scheme which has recently gained steam in literature is the low salinity water flooding which [1] refers to as OPTSWF. The OPTSWF which entails the injection of diluted brine with significantly lower salinity than the connate water, has resulted in reduction in residual oil saturation and consequently increase in recoveries from multiple experiments from different authors around the world [2], [3].

To capture the potentials from OPSWF, several authors have carried out laboratory studies using progressively diluted brines to flood cores saturated with crude oil [3]. The tests usually monitor the recovered oil, brine and pressure drop across the core with time during the experiment. To assess the potential gains of the OPTSWF scheme in an oilfield, a sector model from the field is built and then, the results from the tests are integrated into the model and then the results are quantitatively assessed.

2.THEORETICAL ANALYSIS

The relative permeability which is a measure of the relative ease with which a fluid moves in a porous medium in the presence of another fluid and is a composite function which is affected by several rock parameters including pore throat geometry, capillary pressure, burial and saturation history, rock and fluid composition etc. [4], [5]. [6]. Corey proposed a method for the determination of relative permeability by making use of fixed oil and water end points, exponents, residual oil and connate water saturation [7].

$$k_{rw} = \left[\frac{S_w - S_{wi}}{1 - S_{wi} - S_{or}} \right]^{nw} \quad (1)$$

$$k_{ro} = \left[\frac{S_o - S_{wi}}{1 - S_{wi} - S_{or}} \right]^{no} \quad (2)$$

By keeping all other parameters constant and changing the residual oil saturations from the pre-OPTSWF to the post-OPTSWF core flood results, relative permeability curves for different salinity levels can be derived. These curves can then be entered into a simulator to model the reservoir performance for comparison over a given duration. The key upscaling method used from laboratory to the field sector scale is the relative permeability curves which is derived from the core flooding experiment. The relative permeability curve is a composite rock-fluid property and is a function of interfacial tension, wettability, capillary pressure, pore size structure, mineralogy, salinity [1]. It is this composite property which is used to upscale the results from the core scale to the field scale. It is important to point out that fluid and rock properties are the same both at the core and field scale. However, at the field scale, there may be a higher level of heterogeneity in the rock properties. To manage the heterogeneity at the field scale, the reservoir is divided into flow units or rock types and for each rock type or flow unit, a corresponding core plug is obtained, and the experiments are run on such core plugs and then transferred to the field model.

3.MATERIALS AND METHODS

The input data for this study was sourced from [8], these are presented in Table - Table 2 and Figure 1 - Figure 2.

Table 1. Core Plug Properties

Experiment Number	Core Length	Diameter	PV	PHI	Swi	SorHS	SorLS
EXPERIMENT 7	2.50	3.80	5.80	20%	12%	38%	16%

Table 1. Oil-Water Relative Permeability Tables for High Salinity and Low Salinity Core Flooding

HS					LS				
Sw	SWC	SOC	KRW_HS	KRO_HS	Sw	SWC	SOC	KRW_HS	KRO_HS
12.07%	0.00%	100.00%	0.00	0.85	12.07%	0.00%	100.00%	0.00	0.85
14.57%	5.00%	95.00%	0.00	0.75	14.57%	3.45%	96.55%	0.00	0.78
17.07%	10.00%	90.00%	0.00	0.65	17.07%	6.91%	93.09%	0.00	0.71
19.57%	15.00%	85.00%	0.00	0.57	19.57%	10.36%	89.64%	0.00	0.65
22.07%	20.00%	80.00%	0.00	0.49	22.07%	13.81%	86.19%	0.00	0.59
24.57%	25.00%	75.00%	0.01	0.41	24.57%	17.26%	82.74%	0.00	0.53
27.07%	30.00%	70.00%	0.01	0.35	27.07%	20.72%	79.28%	0.00	0.48
29.57%	35.00%	65.00%	0.02	0.29	29.57%	24.17%	75.83%	0.01	0.43
32.07%	40.00%	60.00%	0.03	0.24	32.07%	27.62%	72.38%	0.01	0.38
34.57%	45.00%	55.00%	0.04	0.19	34.57%	31.07%	68.93%	0.01	0.34
37.07%	50.00%	50.00%	0.05	0.15	37.07%	34.53%	65.47%	0.02	0.29
39.57%	55.00%	45.00%	0.07	0.12	39.57%	37.98%	62.02%	0.02	0.26
42.07%	60.00%	40.00%	0.09	0.09	42.07%	41.43%	58.57%	0.03	0.22
44.57%	65.00%	35.00%	0.11	0.06	44.57%	44.88%	55.12%	0.04	0.19
47.07%	70.00%	30.00%	0.14	0.04	47.07%	48.34%	51.66%	0.05	0.16
49.57%	75.00%	25.00%	0.17	0.03	49.57%	51.79%	48.21%	0.06	0.14
52.07%	80.00%	20.00%	0.20	0.02	52.07%	55.24%	44.76%	0.07	0.11
54.06%	85.00%	15.00%	0.25	0.01	54.06%	58.69%	41.31%	0.08	0.09
57.07%	90.00%	10.00%	0.29	0.00	57.07%	62.15%	37.85%	0.10	0.07
59.57%	95.00%	5.00%	0.34	0.00	59.57%	65.60%	34.40%	0.11	0.06
62.07%	100.00%	0.00%	0.40	0.00	62.07%	69.05%	30.95%	0.13	0.05
					64.57%	72.50%	27.50%	0.15	0.03
					67.07%	75.96%	24.04%	0.18	0.02
					69.57%	79.41%	20.59%	0.20	0.02
					72.07%	82.86%	17.14%	0.23	0.01
					74.57%	86.31%	13.69%	0.26	0.01
					77.07%	89.77%	10.23%	0.29	0.00
					79.57%	93.22%	6.78%	0.32	0.00
					82.07%	96.67%	3.33%	0.36	0.00
					84.40%	99.89%	0.11%	0.40	0.00

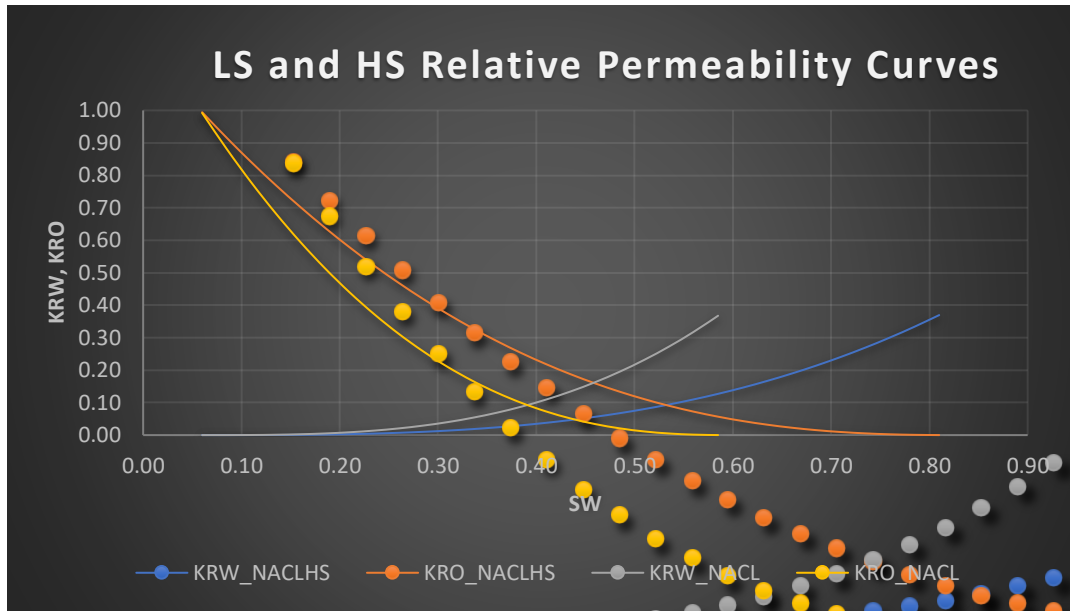


Figure 1. Oil-Water Relative Permeability Curves for HS and LS Core Flooding

3.1. Synthetic Grid

A synthetic cartesian grid was also built using a black oil simulator. The grid properties are summarized in Figure 2 and Table 2. A homogenous grid with uniform properties has been selected for this study as enumerated in Table 2. This assumption can be validated in upper shoreface depositional environment reservoirs where bulky sands with generally uniform properties are dominant.

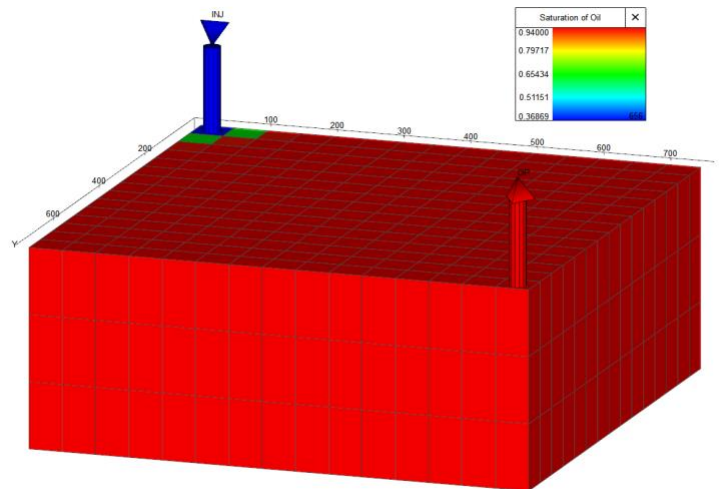


Figure 2. Synthetic Grid Used for Study

Table 2. Properties of Synthetic Cartesian Grid

Property	Value
Dimensions (X*Y*Z)	15*15*3
STOIP, mmSTB	67
Porosity, %	27
PermX=PermY, md	1000
PermZ, md	100
Oil Producer(s)	1
Water Injectors(s)	1
Oil Production Rate, stb/d	12,580
Water Injection Rate, sbt/d	12,580
Simulation Start Date (dd.mm.yyyy)	01.01.1990
Simulation End Date (dd.mm.yyyy)	31.12.2015
Oil Water Contact, ftss	2700
Pay Thickness, ft	25
Oil FVF, rb/stb	1.2
Oil Viscosity, cp	0.47

3.2. Cases Considered

The following cases were simulated and using the synthetic grid.

- i. Secondary Mode: HS Flooding (10,000 ppm NACL)
- ii. Secondary Mode: HS Flooding (5,000 ppm NACL)
- iii. Secondary Mode: HS Flooding (2,500 ppm NACL)
- iv. Secondary Mode: HS Flooding (1,250 ppm NACL)
- v. Secondary Mode: HS Flooding (625 ppm NACL)

Secondary water injection with 10,000 ppm NACL is the base case. This is the conventional water injection mode. In this base case mode, the initially oil saturated cartesian grid shown in Figure 2 was flooded with HS brine (10,000 ppm). For the subsequent cases, the salinity of the invading brine is reduced by half.

4. RESULTS AND DISCUSSION

The results for all cases considered are presented in Figure 3 to Figure 16. It is to be noted that as the salinity of the brine is reduced, additional oil is mobilized as seen from the relative permeability curves in Figure 1. This additional oil recovered is obtained because of a reduction in the residual oil saturation from the higher salinity flood. [3] Pointed out that as the salinity of the invading brine is reduced below that of the connate brine, an initial equilibrium which exists between the crude-brine-rock is destabilized, and this leads to the mobilization of some residual oil.

Key Findings

1. The comparative performance plot shown in Figure 15 reveals that the plateau life and cumulative oil is improved as the salinity of the flooding brine is reduced. This is very interesting to note as many brown fields can potentially benefit from this scheme.
2. Also, the saturation profile shown in Figure 16 depicts the improved sweep efficiency as the salinity is reduced. The flood front moves slower through the model and the hydrocarbon saturation behind the flood is observed to be lower with reducing water salinity.
3. Optimum salinity water flooding can be employed in the secondary mode to brown fields right from the onset of development to enhance the additional recoveries producible from the field.

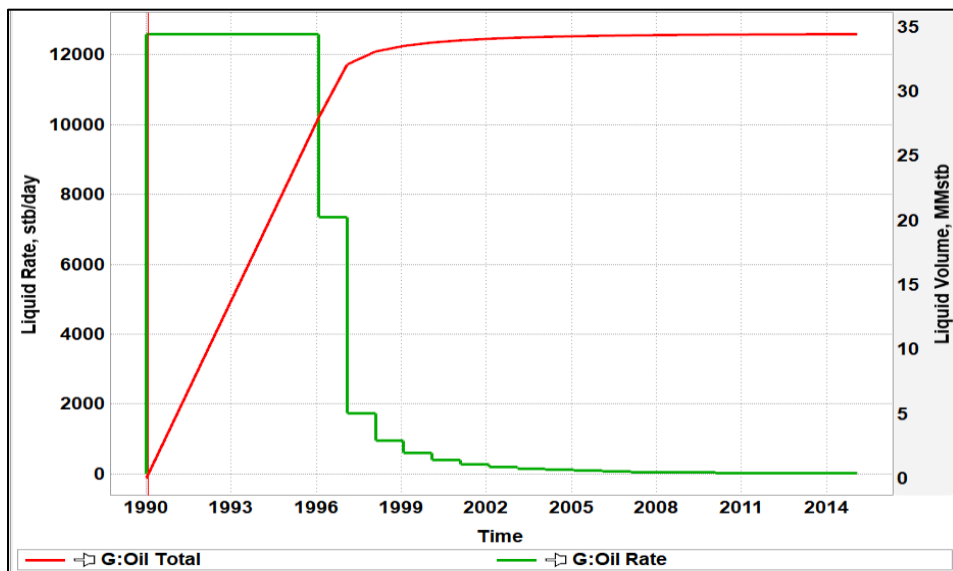


Figure 3. Production Performance - Secondary Mode: HS Flooding (10,000 ppm NACL)

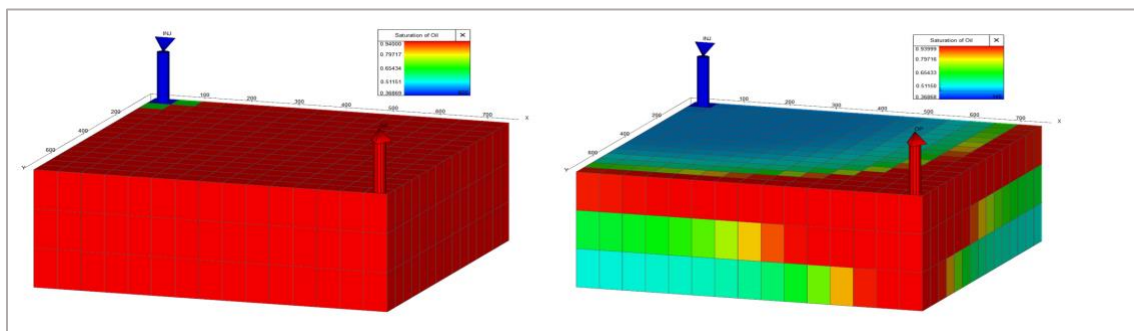


Figure 4. Pre (left) and Postproduction (Right) Saturation Distribution - Secondary Mode: HS Flooding (10,000 ppm NACL)

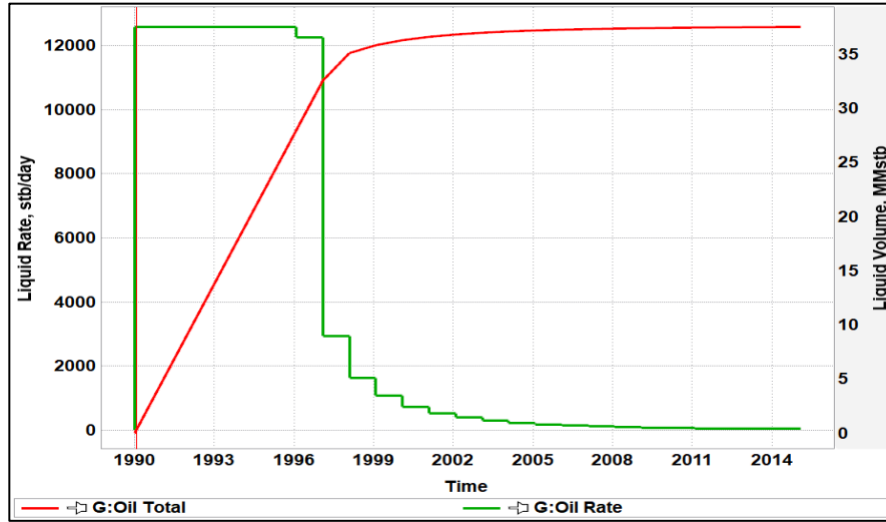


Figure 5. Production Performance - Secondary Mode: HS Flooding (5,000 ppm NACL)

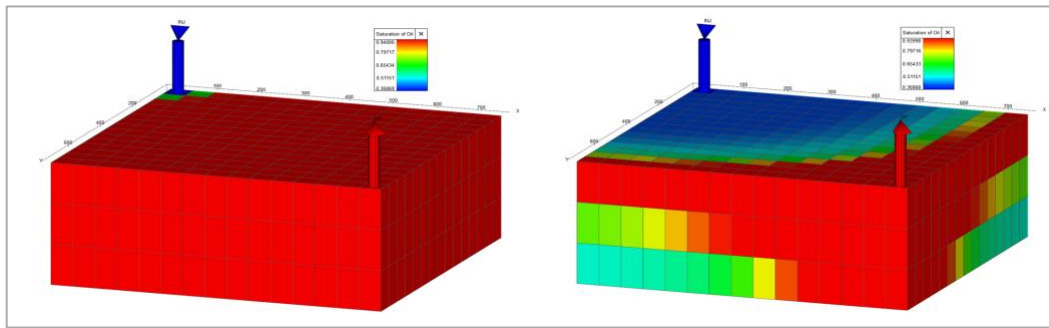


Figure 6. Pre (left) and Postproduction (Right) Saturation Distribution - Secondary Mode: HS Flooding (5,000 ppm NACL)

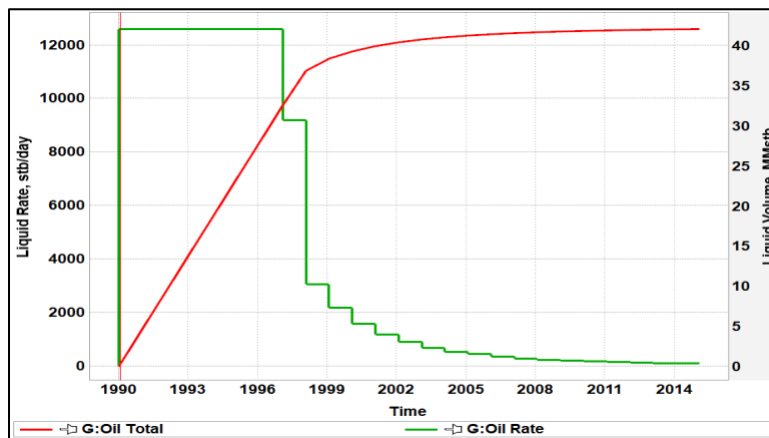


Figure 7. Production Performance - Secondary Mode: HS Flooding (2,500 ppm NACL)

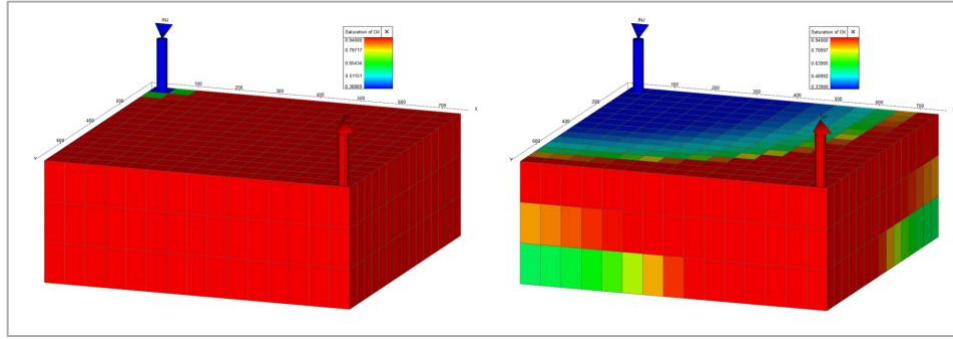


Figure 8. Pre (left) and Postproduction (Right) Saturation Distribution - Secondary Mode: HS Flooding (2,500 ppm NACL)

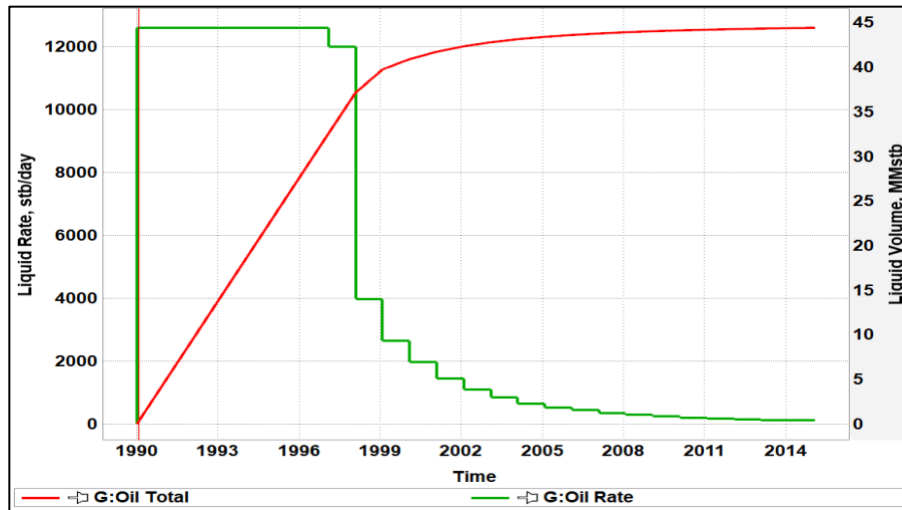


Figure 9. Production Performance - Secondary Mode: HS Flooding (1,250 ppm NACL)

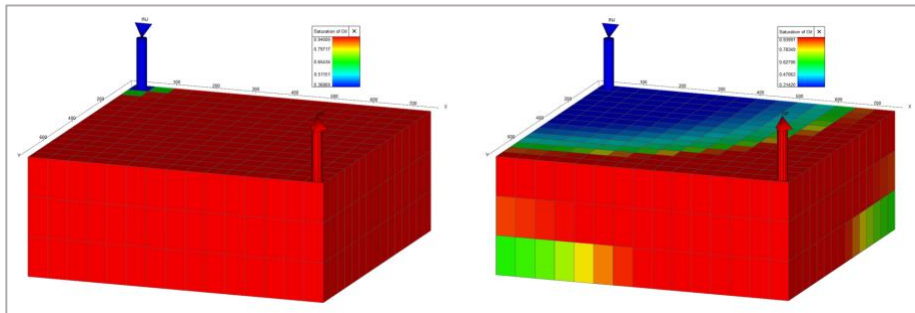


Figure 10. Pre (left) and Postproduction (Right) Saturation Distribution - Secondary Mode: HS Flooding (1,250 ppm NACL)

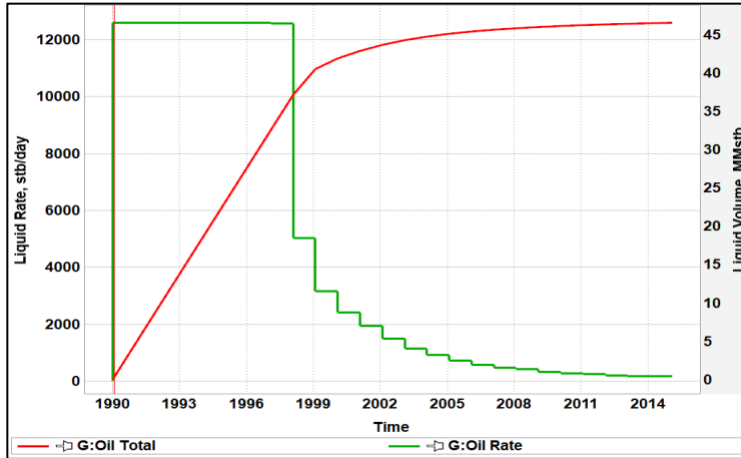


Figure 11. Production Performance - Secondary Mode: HS Flooding (625 ppm NACL)

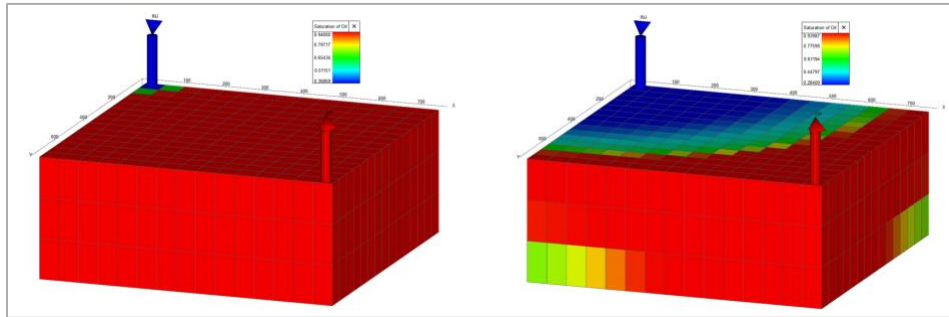


Figure 12. Pre (left) and Postproduction (Right) Saturation Distribution - Secondary Mode: HS Flooding (625 ppm NACL)

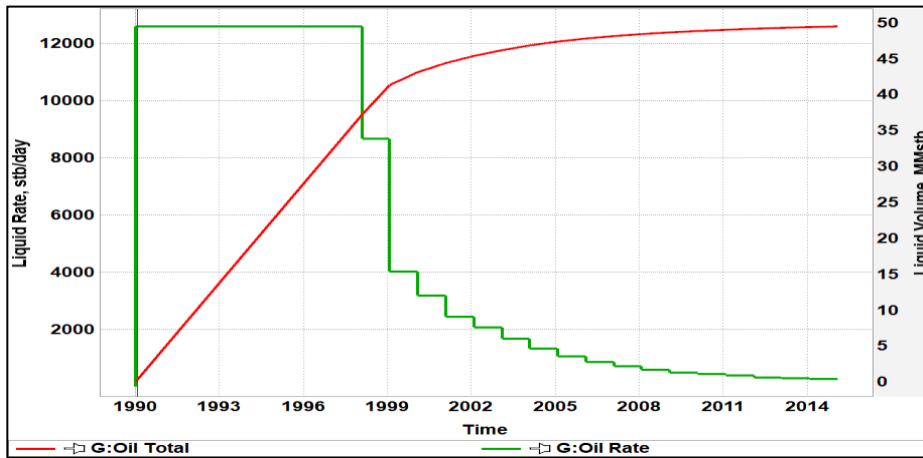


Figure 13. Production Performance - Secondary Mode: HS Flooding (0 ppm NACL)

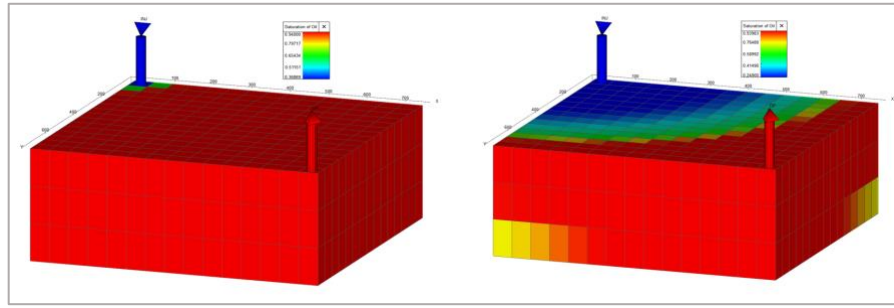


Figure 14. Pre (left) and Postproduction (Right) Saturation Distribution - Secondary Mode: HS Flooding (0 ppm NACL)

Comparative Plot

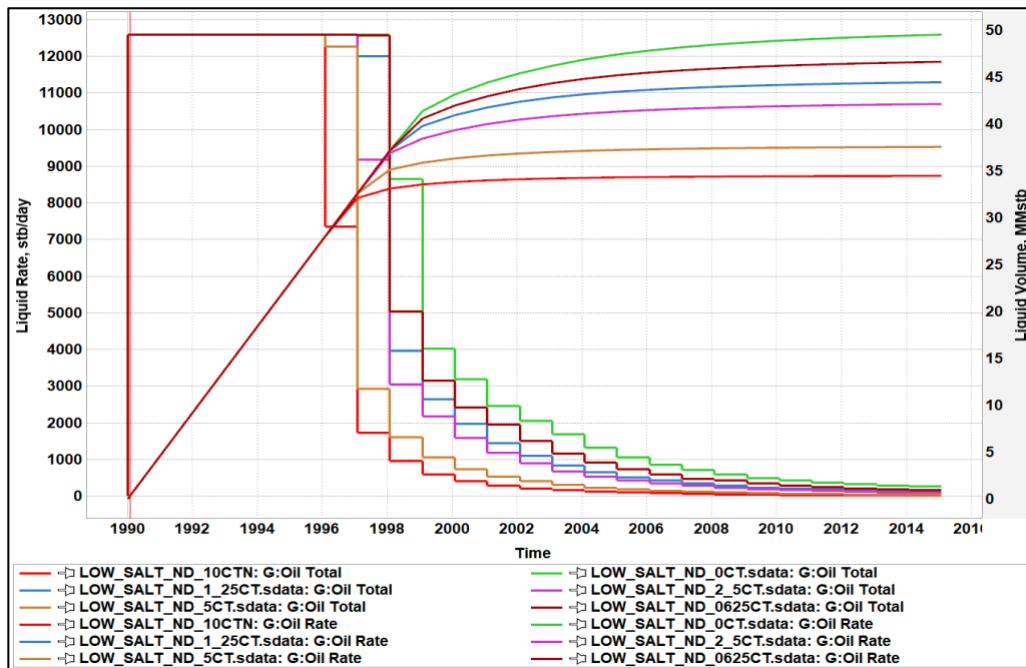


Figure 15. Production Performance - Secondary Mode: HS Flooding (All Cases)

5. CONCLUSION

This work has integrated the results from core flooding experiments with a synthetic 3D grid to visualize and quantify the performance of progressively reducing salinity waterflooding employed in the secondary mode.

- I. Additional oil recoveries ranging from 3 mmstb to ~9mmstb were produced in the 5000 ppm and 0 ppm flooding mode compared to the 10,000-ppm secondary flooding mode Figure 15.
- II. Also, the water breakthrough time is increased due to the improved sweep efficiency, thus resulting in increased well and field life. The field life is enhanced by an additional 1-2 years Figure 15.

III. Again, the result from this work also enables the visualization of the movement of the flood front and the sweep efficiency Figure 16. This implies that the microscopic sweep efficiency is enhanced as the residual oil saturation to water is further reduced.

Additional areas which can be explored for further studies include.

- a) Exploring the performance of low salinity waterflooding in the tertiary mode to demonstrate potential application to brown fields
- b) Carry out detailed economic analysis to sense check the cost/benefit analysis from implementing the low salinity water flooding scheme in a typical offshore environment. This will give a sense of required additional unit operating costs and CAPEX, breakeven crude oil price, NPV, IRR, pay back time and other economic indicators.

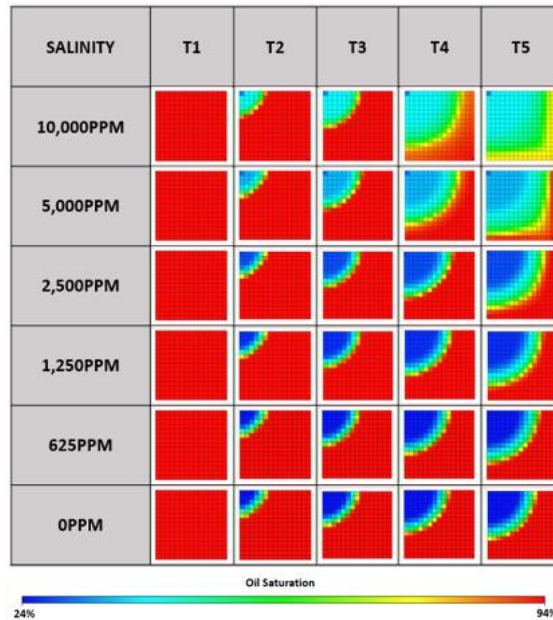


Figure 16. Pre (left) and Postproduction (Right) Saturation Distribution - Secondary Mode: All Cases

Acknowledgements

The authors would like to thank the Nigerian Upstream Petroleum Regulation Agency, Platform Petroleum, Pillar Oil and the Petroleum Engineering Laboratories of Covenant University and University of Ibadan.

Nomenclature

2D:	Two Dimensional
3D:	Three Dimensional
CAPEX:	Capital Expenditure
HS:	High Salinity
HSWF:	High Salinity Waterflooding
IRR:	Internal Rate of Return
Kro:	Relative Permeability to Oil
Krw:	Relative Permeability to Water
LS:	Low Salinity

LSWF:	Low Salinity Waterflooding
No:	Oil Corey Exponent
NPV:	Net Present Value
Nw:	Water Corey Exponent
OPEX:	Operational Expenditure
OPSWF:	Optimum Salinity Waterflooding
PHI:	Effective Porosity
PV:	Pore Volume
Soc:	Normalized Corey Oil Saturation
Sorw:	Residual Oil Saturation
Sorw_HS:	Residual Oil Saturation under High Salinity
Sorw_LS:	Residual Oil Saturation under Low Salinity
Swc:	Normalized Corey Water Saturation
Swi:	Connate Water Saturation
mmSTB:	Million Stock Tank Barrels
STOIP:	Stock Tank Original Oil in Place

REFERENCES

- [1] O. O. O. O. David Alaigba, "Optimized Salinity Water Flooding as an Improved Oil Recovery IOR Scheme in the Niger Delta," in *SPE Nigeria Annual International Conference and Exhibition, August 11–13, 2020, Lagos, 2020*.
- [2] J. Sheng, "Critical review of low-salinity waterflooding," *Journal of Petroleum Science and Engineering*, vol. 120, no. ISSN 0920-4105, pp. 216-224, 2014.
- [3] F. S. Allan Katende, "A critical review of low salinity water flooding: Mechanism, laboratory and field application," *Journal of Molecular Liquids*, vol. 278, no. ISSN 0167-7322, pp. 627-649, 2019.
- [4] T. G. Sorop, S. K. Masalmeh, B. M. Suijkerbuijk, H. A. v. d. Linde, H. Mahani, N. J. Brussee, F. A. Marcelis and A. Coorn, "Relative Permeability Measurements to Quantify the Low Salinity Flooding Effect at Field Scale," in *Abu Dhabi International Petroleum Exhibition and Conference, Abu Dhabi, UAE, November 2015*, Abu Dhabi, 2015.
- [5] J. H. L. ., A. E. a. K. D. S. Faisal Awad Aljuboori, "Using Low Salinity Waterflooding to Improve Oil Recovery in Naturally Fractured Reservoirs," *Appl. Sci.*, vol. 10, no. 12, 2020.
- [6] O. O. O. O. David Alaigba, "Correlations for Estimating Change in Residual Oil Saturation During Low Salinity Water Flooding," *International Journal of Engineering and Innovative Research*, vol. 3, no. 2, pp. 101-114, 2021.
- [7] R. N. C. S. G. M. K. L. W. A. R. T. C. W. a. H. N. Horne, "Steam-Water Relative Permeability," in *World Geothermal Congress, Kyushu-Tohoku, Japan, 28 May to 10 June, Tokyo, 2000*.
- [8] O. O. O. O. Alaigba David, "Correlations for Estimating Reduction in Residual Oil Saturation During Low Salinity Waterflooding," *International Journal of Engineering and Innovative*, vol. 3, no. 2, pp. 101-114, 2021.